

# Nonequilibrium orders in parametrically driven field theories

Carl Philipp Zelle,<sup>1</sup> Romain Daviet,<sup>1</sup> Andrew J. Millis,<sup>2,3</sup> and Sebastian Diehl<sup>1</sup>

<sup>1</sup>*Institut für Theoretische Physik, Universität zu Köln, 50937 Cologne, Germany*

<sup>2</sup>*Center for Computational Quantum Physics, The Flatiron Institute, 162 5th Avenue, New York, NY 10010*

<sup>3</sup>*Department of Physics, Columbia University, 538 West 120th Street, New York, New York 10027*

(Dated: June 24, 2025)

Driving quantum materials with coherent light has proven a powerful platform to realize a plethora of interesting phases and transitions, ranging from ferroelectricity to superconductivity and limit cycles in pumped magnonics. In this paper we develop the field theoretical framework to describe nonequilibrium phases that emerge in systems pumped by rapid parametric drives. We consider paradigmatic  $O(N)$  models that describe the long-wavelength fluctuations of ordering fields in many condensed matter set ups. We show that rapid parametric driving of these models can induce an effective pump mechanism in the long wavelength regime through nonlinear scattering. This induces a nonequilibrium transition into a time-crystalline phase.

*Introduction* – The classification and description of nonequilibrium phases of matter as well as their realisations in physical systems are major research endeavors in modern physics [1]. While the mechanisms of phase transitions and their universal behaviors set by dimension and symmetry are (in many cases) well understood in thermal equilibrium [2], the situation is much less clear for nonequilibrium steady-states in driven and open systems.

One of the most prominent resources of nonequilibrium conditions in recent experiments is laser pumping of a material coupled to a bath. In various setups, resonant driving of a high frequency mode can stabilize a macroscopic nonequilibrium steady-state at low frequencies. Examples range from driven-dissipative Bose condensation of exciton-polaritons in cavity pumped materials [3–10] to transient light induced ferroelectricity [11, 12] and superconductivity at temperatures well above the equilibrium superconducting critical temperature [13–17]. Furthermore, pumping magnetic structures leading to driven nonlinear magnonics [18, 19] and magnon condensates observed in laser driven Yttrium-iron-garnet (YIG) films [20, 21] represents a fruitful avenue to create nonthermal phases of matter.

While effective non-equilibrium field theories have successfully been employed to predict non-equilibrium scaling behavior in exciton-polariton condensates [22], a more general understanding of nonequilibrium condensates in field theories of driven materials is lacking. In this letter, we present a general mechanism to induce a condensation into a nonthermal phase with long range order by pumping high frequency degrees of freedom without explicitly breaking any internal symmetries. More concretely, we consider bosonic order parameter theories with a global  $O(N)$  symmetry, the paradigm of continuum descriptions of phases and transitions in condensed matter, as a starting point. A prominent realization is as the theory of magnetic ordering in a Heisenberg model, but it emerges in many contexts [23, 24]. We argue, that once coupled to a thermal bath as well as a fast paramet-

ric pump, these models can exhibit an instability towards a stable nonequilibrium state that manifests as a dynamic limit cycle of a collective order parameter which rotates at a period  $\bar{T}$  much larger than the drive period  $\tau_D \ll \bar{T}$ , and is incommensurate with it.

Such a phase that breaks time translation symmetry, and thus constitutes a so-called time crystal [25, 26], cannot exist in thermal equilibrium where it would constitute a perpetuum mobile [27, 28]. While much effort has been devoted to the realization of discrete time crystals in Floquet systems [29–34], continuous time crystals in driven-dissipative systems have also received a lot of attention [35–38]. Recently, active matter models with continuous time-translation symmetry, where nonreciprocal interactions induce long-range ordered limit cycles, have attracted significant attention [39–45]. This has inspired efforts to engineer drives and dissipation to induce nonreciprocal interactions between microscopic spin degrees of freedom [46, 47] to induce time-crystalline order in quantum material based platforms.

In the following we present analytic derivations and complementary numerical simulations showing how a slow limit cycle phase emerges. We construct the resulting phase diagram and elaborate on the associated critical phenomena.

*Model* – We consider the dynamics of an  $N$ -component bosonic field  $\phi \in \mathbb{R}^N$  with a global  $O(N)$  symmetry in  $d + 1$  dimensions. In a closed system it is described by a Lagrangian

$$\begin{aligned} \mathcal{L}[\phi] &= -\frac{1}{2}\phi^T(\partial_t^2 + Z\vec{\nabla}^2)\phi + V[\phi], \\ V[\phi] &= \frac{1}{2}r\phi^2 + \frac{\lambda}{4}\phi^4. \end{aligned} \quad (1)$$

To capture dynamical and fluctuation effects, we place this Lagrangian on a Keldysh contour. We linearly couple it to a bosonic Ohmic bath describing the cold thermal reservoir for the system. Integrating out this bath, and performing the Keldysh rotation on the time contour  $\phi_{c,q} = 1/2(\phi_+ \pm \phi_-)$  then yields the following dissipative

Keldysh Lagrangian [22, 48]:

$$\mathcal{L}_K[\phi_{c,q}] = -\phi_q^T(\partial_t^2 - Z\vec{\nabla}^2 + 2\gamma\partial_t)\phi_c + 4iD\phi_q^2 - V[\phi_c + \phi_q] + V[\phi_c - \phi_q]. \quad (2)$$

Here  $\gamma$  is the dissipation rate into the thermal bath at temperature  $T = D/\gamma$  (we use units in which  $k_B = 1$ ). We have also dropped non-Markovian contributions that are subleading on the large time scales  $|t - t'| \gg 1/T$  we are interested in [48]. Note that we cannot drop the second order time derivative despite the presence of dissipation, since it is necessary to capture the coherent oscillatory effects potentially present in nonequilibrium phases [19, 41]. We now drive this system parametrically at a fast frequency  $2\Omega$  leading to a time dependent potential  $V[\phi](t)$  through an oscillating mass  $r \rightarrow r(t) = r_0 + r_D \cos 2\Omega t$ . Physically, this is the most generic way in which a microscopic rapid drive not breaking any symmetries can manifest.

Our goal now is to derive a coarse grained effective theory on time scales  $\tau \gg \Omega^{-1}$ , where the dynamics are no longer explicitly time dependent. We first lay out the physical intuition for the effect of the rapidly oscillating parametric drive – importantly, the mechanism does not rely on the specific Lagrangian considered here, but can be adapted to other setups as well: At the linear level, the drive leads to parametric resonance of modes at momenta  $|\mathbf{q}| \sim q_\Omega$ , where their dispersion is  $\omega(q_\Omega) \sim \Omega$ . The far detuned, small frequency modes remain unaffected at that level. This leads to a situation, where the low-frequency spectrum is occupied according to a thermal distribution at the temperature set by the thermal bath, while the parametrically excited modes form a highly occupied reservoir. Beyond the linear level, the reservoir modes then start to scatter and relax into the low frequency regime, dissipating their energy into the thermal bath. They effectively “rain down” into the long wavelength regime constituting an effective incoherent single particle pump. Upon eliminating the reservoir, this manifests as an “antidamping” contribution  $\delta\gamma < 0$ , and a heating effect  $\Delta D > 0$ . This is schematically visualized in Fig. 1a. Note that this heuristics is not limited to pumping high momentum modes as indicated in the figure. It simply requires the existence of a band of high frequency modes, which can be driven parametrically. Furthermore, there needs to be a nonlinear scattering between high and low frequency bands. If the system is coupled to a bath to which it can relax energy – in a material, that would typically be phonons – this is not suppressed by energy conservation.

We now derive this effect analytically for the concrete Lagrangian at hand starting from the symmetric phase,  $r > 0$ . The mechanism also holds for  $r < 0$  as we demonstrate numerically below. Since we are interested in the dynamics at long time scales, noise fluctuations will dominate, and we can take a semiclassical limit of the Keldysh

path integral [48, 49]. It reduces to an MSRJD path integral [50–52] and is equivalent to the Langevin equation

$$\left(\partial_t^2 + 2\gamma\partial_t + r(t) - Z\nabla^2 + \lambda|\phi|^2\right)\phi + \xi = 0. \quad (3)$$

Here,  $\xi$  is a Gaussian white noise whose width is given by  $\langle \xi_i(t, \mathbf{x}), \xi_j(t', \mathbf{x}') \rangle = D\delta(t - t')\delta(\mathbf{x} - \mathbf{x}')$ . To eliminate the high frequency reservoir modes created by the rapid drive, we split the field  $\phi(t, \mathbf{x})$  into the slow, low momentum degrees of freedom  $\phi_{<}(t, \mathbf{x})$ , and the fast reservoir modes  $\phi_{>}(t, \mathbf{x})$  that predominantly occupy a momentum shell at  $q_\Omega$ . The momentum-dependent Keldysh Green’s functions are dominated by the reservoir momenta with occupation density  $n_b$ , which is set by the pump power. We can now integrate out the fast modes leading to an effective theory for the low frequency degrees of freedom through loop corrections. We do this to leading order in a perturbative loop expansion:

$$\delta\gamma = -\mathcal{N}_\gamma \lambda^2 (q_\Omega n_b)^2, \quad (4)$$

$$\Delta D = \frac{\lambda^2}{\Omega^2} \mathcal{N}_D (q_\Omega n_b)^3. \quad (5)$$

Here we focus on the dependence on the most relevant tuning knobs, while  $\mathcal{N}_{\gamma,D} > 0$  collect model constants and are provided in the SM, where we also elaborate on the details of the calculation. This yields two important takeaways: (i) The highly occupied reservoir indeed yields an antidamping effect since  $\delta\gamma < 0$ , (ii) for very strong drive powers, the induced noise  $\Delta D$  dominates over the single particle pumping and will destroy any ordering tendencies. Importantly however, if the initial dissipation  $\gamma$  is small enough, it is possible to achieve  $|\delta\gamma| > \gamma$ , so that the effective damping  $\gamma_{\text{eff}} = \gamma + \delta\gamma$  is tuned through zero. This triggers an instability towards a limit cycle phase, where the order parameter  $\langle \phi \rangle$  is dynamically rotating on a circle [41], e.g., for  $N = 3$

$$\langle \phi(t) \rangle = \phi_0 (\cos \omega_0 t, \sin \omega_0 t, 0)^T. \quad (6)$$

This phase is stabilized by nonlinear damping forces  $\propto u|\phi|^2\partial_t\phi$  that are generated by the reservoir coupling, too, as we show in the supplement. If the drive strength is too large however, the heating effect will destroy any long-range order. The resulting phase diagram is sketched in Fig. 1b.

*Pumped magnetic materials*– An important physical example, where our mechanism could be put to test, is an isotropic antiferromagnet. For instance, the cubic lattice Hubbard model at half filling, is well described by a bosonic  $O(3)$  symmetric field theory with dynamical exponent  $z = 1$  on a mesoscopic level [23, 53]. To describe the long wavelength spectrum of the antiferromagnetically ordered phase, the respective field theory has to be in the ordered phase in equilibrium, i.e.  $r < 0$  in Eq. (1). In the case of a Hubbard model at half filling with strong interaction  $|r| \sim zt^2/U$ , where  $t$  is the Hopping,  $U$  the

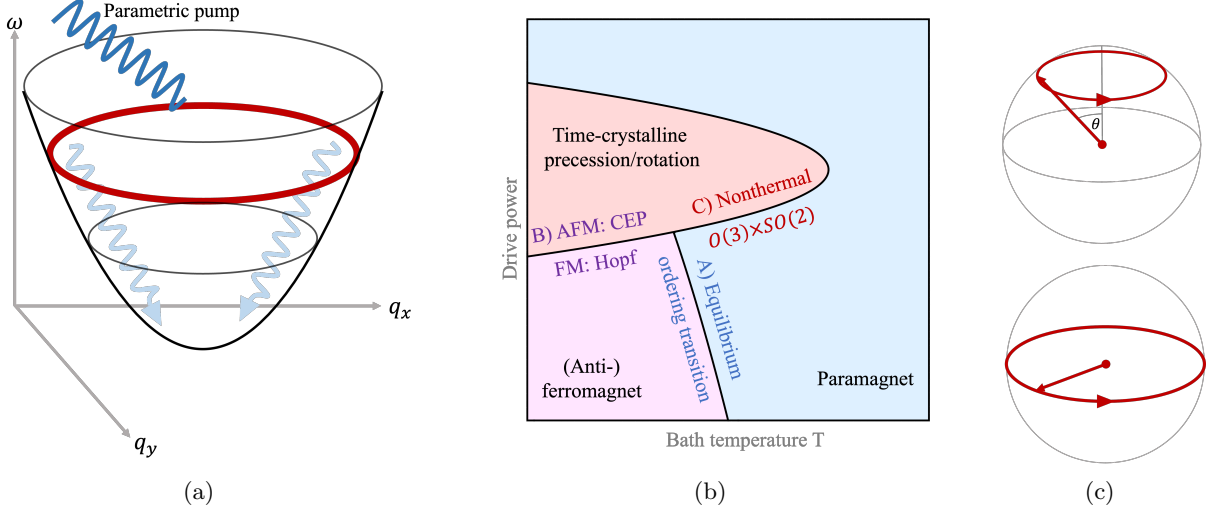


FIG. 1: Left panel: Sketch for magnon pump scheme. Middle panel: Schematic phase diagram of the driven (anti-)ferromagnet with bath temperature  $T$  and pumping reservoir occupation  $n_b$ . At small drives there are the two static phases, paramagnet and antiferro- or ferromagnet for positive or negative Heisenberg coupling  $J$ , respectively. At suitably strong drives and low noise levels, time crystalline order emerges. Too strong drives induce heating and push the system back in a thermal paramagnetic state. Right panel: visualization of time crystalline orders. Rotation for antiferromagnet (AFM) and precession for Ferromagnet (FM).

Hubbard repulsion and  $z$  the lattice coordination number. The closed system ( $\gamma = 0$ ) then has two gapless Goldstone excitations transversal to the ordering vector with ballistic dispersions  $\omega_T(\mathbf{q} = 0) = \pm v|\mathbf{q}|$  and velocity  $v = \sqrt{Z}$ . The longitudinal fluctuations have a frequency gap of  $\Delta_L = 2|r|$ . The remaining potential parameter  $\lambda$  sets the scattering length of magnetic excitations. All these parameters can in principle be either computed from an underlying electronic model, like the Hubbard model in a strong coupling expansion, or determined experimentally to fix the effective model.

Phononic baths generically give rise to thermal noise fluctuations and dissipation at a fixed temperature, so that neither energy nor total magnetization are conserved. These can be modeled by dissipation and noise rates  $\gamma(\mathbf{q})$  and  $D(\mathbf{q})$  with a potential momentum dependence that still obeys fluctuation-dissipation relations of thermal equilibrium,  $\gamma(\mathbf{q})/D(\mathbf{q}) = \text{const.}$  They typically increase monotonically with momentum  $\mathbf{q}^2$ , since there is more phase space for scattering with bath degrees of freedom. It is typically modeled to leading order in  $\mathbf{q}^2$ . The zero momentum mode of the dissipation,  $\gamma(\mathbf{q} = 0)$ , gives the decay rate of the total  $O(N)$  charge (e.g. magnetization) of the system, while energy is dissipated at all momenta.

Parametric drives can arise, for instance, through oscillating electric fields. On the level of the Hubbard model, these parametrically drive the hopping via Peierls substitution [54]. If this drive's frequency is below the Mott gap, it does not create electronic excitations and the dynamics is still well described by local magnetic mo-

ments. It then carries through as a parametric drive into the continuum limit. With that one arrives at the Lagrangian (2) as the continuum theory of the strongly coupled Hubbard model at half filling, coupled to a cold bath and pumped by oscillating electric fields albeit in the ordered sector ( $r < 0$ ).

While the analytic derivations shown above were performed by driving the symmetric phase,  $r > 0$ , the pumping mechanism is not restricted to that regime. The parametric drive may be tuned to excite high momentum transversal modes or directly address the gapped longitudinal modes at  $\Omega = 2\Delta_L$  to create a high frequency reservoir that pumps the gapless transversal modes through scattering processes. Importantly, the parametric pumping does not break any of the system's symmetries and hence cannot gap out the Goldstone excitations. Note that a Floquet RPA analysis of such a Hubbard model in the strong coupling regime at half-filling and driven by oscillating electric fields indeed yields numerical evidence of a nonequilibrium phase transition occurring [54, 55]. We conjecture that this 'magnon condensation' is precisely the onset of the nonequilibrium time-crystal we describe here.

We also highlight the important special case of an  $SO(3)$  symmetry group (as distinct from  $O(3)$  discussed above), describing isotropic ferromagnets, for example. In this case, an additional symmetry allowed cubic coupling contributes to the Lagrangian, of the form

$$\kappa \phi_q \cdot (\partial_t \phi_c \times \phi_c). \quad (7)$$

This coupling changes the limit cycle itself from a rota-

tion on a grand circle to a precession of the form

$$\langle \phi(t) \rangle = \phi_0 (\sin \theta \cos \omega_0 t, \sin \theta \sin \omega_0 t, \cos \theta)^T, \quad (8)$$

where the precession angle reaches  $\theta \rightarrow \pi/2$ , corresponding to rotation on a circle, as  $\kappa \rightarrow 0$ . It furthermore alters the loop structure of the scattering between reservoir and long wavelength modes but does not change the essential property  $\delta\gamma < 0$ , see supplemental material. The dynamic limit cycles are visualized in Fig. 1c

*Universal scaling* – Let us now briefly describe the universality classes associated to the nonequilibrium transitions triggered by tuning the damping through zero in the effective nonequilibrium  $O(N)$  model (2). In the  $O(3)$  symmetric case, this reproduces the universality classes discussed in [41, 56]. The transition from the symmetric phase  $r > 0$  falls into a nonequilibrium universality class, where the universal scaling of correlations and responses violates fluctuation-dissipation relations. The transition from the ordered phase,  $r < 0$ , into the nonequilibrium time crystal is described by a so-called critical exceptional point (CEP). It leads to giant fluctuations [41, 57], which either suppresses the existing order or triggers a fluctuation-induced weakly first-order transition [41].

In the case of an  $SO(3)$  symmetric theory, we show in the SM that the additional coupling (7) is irrelevant at the  $r > 0$  transition, and does not alter the universality class. This is however different as one approaches the time-crystalline phase starting from an ordered phase. There is no CEP in this case, and the transitions realizes a noisy Hopf bifurcation as we show in the SM. The transition falls into the equilibrium  $O(2)$  universality class [58–61].

*Numerics* – Our analytical derivations suggest that the parametrically pumped, dissipative  $O(N)$  model hosts a stable nonequilibrium state in the form of a slow limit cycle phase. We now corroborate these results by direct numerical simulations. To that end, we simulate the Langevin equation (3) with an explicitly time dependent  $r(t)$ . Mimicking an antiferromagnet, we perform these simulations at  $r < 0$ , as explained above. The spin-wave velocity is set to unity and we assume very small Gilbert dampings. Simulations on a cubic lattice of length  $L = 32$  show, that indeed initially a sufficient drive induces a high occupation of longitudinal modes at momenta  $q_\Omega$ . These however quickly scatter into the low momentum/frequency regime, and lead to a macroscopic occupation of transversal modes at  $\mathbf{q} = 0$ , and at a finite frequency  $\omega_0$ . As predicted theoretically, there is a coherent, long range ordered rotation of the order parameter, visualized in Fig 2a. Along the transition between antiferromagnet and time crystalline order, the mapping to the critical exceptional point of driven  $O(N)$  models predicts a decrease of the amplitude at the transition due to the exceptionally enhanced fluctuations and a square root behavior of the angular velocity upon penetrating

the rotating phase [41]. Both is confirmed by the numerical simulations as shown in Fig 2.

*Discussion and Outlook*– In this paper, we have presented a universal mechanism to capture nonequilibrium condensation phenomena within parametrically driven, open field theories. Technically, it provides a method to model pumping effects stemming from rapidly oscillating drives effectively by noisy, non-Hermitian field theories that feature an effective time translation invariance on the ‘mesoscopic’ scale of description, but manifestly break equilibrium conditions. In these effective theories, the transition is triggered by tuning an effective damping rate through zero. While our analysis is based on an  $O(N)$  symmetric Lagrangian, the mechanism is more general and applies to other symmetry groups as well. Such a symmetry analysis and the ensuing effective field theory should also describe the universal behavior of magnon condensation in parametrically driven anisotropic magnets [20, 21, 62].

The macroscopic limit cycle characterizing the nonequilibrium phases breaks the effective time translation symmetry of the  $O(N)$  model spontaneously, and thus constitutes a dissipative time crystal. Our theory indicates that such phases can be realised by simple driving schemes in magnetic materials if the damping rate of the undriven system is small. This complements recent approaches to generate limit cycle phases in magnetic systems with lower symmetry [41] and through inducing nonreciprocal interactions of the microscopic spins through engineered drive and dissipation protocols [46, 47].

Further, scaling laws within the time-crystalline phase can be expected to qualitatively deviate from equilibrium phenomenology. On the one hand, in analogy to driven-dissipative exciton polariton condensation, there will be a mode with a Kardar-Parisi-Zhang (KPZ) nonlinearity which leads to subdiffusive transport [63]. It will however interact with the soft modes from the broken internal symmetries paving the way to new nonthermal fixed points in the respective nonlinear sigma models. Additionally, recent work on similar phases in  $O(2)$  ferrimagnets in one dimension has shown that these can constitute ‘active magnets’ with self propelled defects, whose relaxational dynamics differs starkly from equilibrium physics [64].

*Acknowledgments*– We thank A. Chakraborty, R. Hanai, M. Kalthoff, J. Lang, A. Rosch and R. Tazai for useful discussions. We acknowledge support by the Deutsche Forschungsgemeinschaft (DFG, German Research Foundation) CRC 1238 project C04 number 277146847.



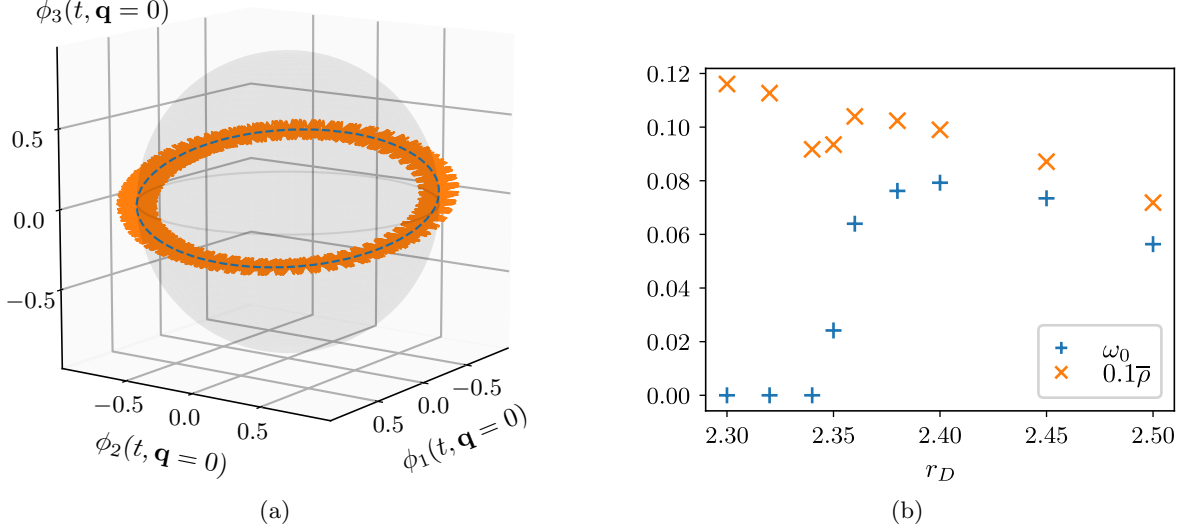


FIG. 2: Numerical simulations of Eq. (3) with  $-r_0 = Z = 1$ ,  $\lambda = 0.5$ ,  $2\gamma = 10^{-3}$  and  $T = 0$  and full  $O(3)$  symmetry,  $\kappa = 0$ . The driving frequency  $\Omega = 2.15$  is chosen to have a parametric resonance of the longitudinal mode around momentum  $q_\Omega \sim \pi/2$ . (a) The long time solution with  $r_D = 2.4$  is given by the orange solid line. The blue dashed line shows the same trajectories averaged over the fast amplitude oscillations (with frequency  $\Omega$ ). The order parameter indeed traces out a circle. (b) Frequency of the limit cycle  $\omega_0$  (blue) and its amplitude  $\bar{\rho}$  (orange) averaged over the fast oscillations as a function of the driving power  $r_D$ . We see that at the transition from ordered to rotating phase, the amplitude dips, which is in line with the critical exceptional point scenario for the transition (see main text).

- 
- [1] U. C. Täuber, *Critical Dynamics* (Cambridge University Press, 2014).
- [2] J. Zinn-Justin, *Quantum Field Theory and Critical Phenomena* (Oxford University Press, 2002).
- [3] A. Imamoglu, R. J. Ram, S. Pau, and Y. Yamamoto, Nonequilibrium condensates and lasers without inversion: Exciton-polariton lasers, *Physical Review A* **53**, 4250–4253 (1996).
- [4] J. Kasprzak, M. Richard, S. Kundermann, A. Baas, P. Jeambrun, J. M. J. Keeling, F. M. Marchetti, M. H. Szymańska, R. André, J. L. Staehli, V. Savona, P. B. Littlewood, B. Deveaud, and L. S. Dang, Bose–einstein condensation of exciton polaritons, *Nature* **443**, 409–414 (2006).
- [5] R. Balili, V. Hartwell, D. Snoke, L. Pfeiffer, and K. West, Bose–einstein condensation of microcavity polaritons in a trap, *Science* **316**, 1007–1010 (2007).
- [6] H. Deng, G. Weihs, C. Santori, J. Bloch, and Y. Yamamoto, Condensation of semiconductor microcavity exciton polaritons, *Science* **298**, 199–202 (2002).
- [7] Q. Fontaine, D. Squizzato, F. Baboux, I. Amelio, A. Lemaître, M. Morassi, I. Sagnes, L. L. Gratiet, A. Harouri, M. Wouters, I. Carusotto, A. Amo, M. Richard, A. Minguzzi, L. Canet, S. Ravets, and J. Bloch, Kardar–parisi–zhang universality in a one-dimensional polariton condensate, *Nature* **608**, 687 (2022).
- [8] T. Byrnes, N. Y. Kim, and Y. Yamamoto, Exciton–polariton condensates, *Nature Physics* **10**, 803–813 (2014).
- [9] H. Deng, H. Haug, and Y. Yamamoto, Exciton-polariton bose-einstein condensation, *Reviews of Modern Physics* **82**, 1489–1537 (2010).
- [10] I. Carusotto and C. Ciuti, Quantum fluids of light, *Rev. Mod. Phys.* **85**, 299 (2013).
- [11] T. F. Nova, A. S. Disa, M. Fechner, and A. Cavalleri, Metastable ferroelectricity in optically strained sr tio 3, *Science* **364**, 1075–1079 (2019).
- [12] X. Li, T. Qiu, J. Zhang, E. Baldini, J. Lu, A. M. Rappe, and K. A. Nelson, Terahertz field–induced ferroelectricity in quantum paraelectric sr tio 3, *Science* **364**, 1079–1082 (2019).
- [13] D. Fausti, R. I. Tobey, N. Dean, S. Kaiser, A. Dienst, M. C. Hoffmann, S. Pyon, T. Takayama, H. Takagi, and A. Cavalleri, Light-induced superconductivity in a stripe-ordered cuprate, *Science* **331**, 189–191 (2011).
- [14] M. Mitrano, A. Cantaluppi, D. Nicoletti, S. Kaiser, A. Perucchi, S. Lupi, P. Di Pietro, D. Pontiroli, M. Riccò, S. R. Clark, D. Jaksch, and A. Cavalleri, Possible light-induced superconductivity in k3c60 at high temperature, *Nature* **530**, 461–464 (2016).
- [15] K. A. Cremin, J. Zhang, C. C. Homes, G. D. Gu, Z. Sun, M. M. Fogler, A. J. Millis, D. N. Basov, and R. D. Averitt, Photoenhanced metastable c-axis electrodynamics in stripe-ordered cuprate la1. 885ba0. 115cuo4, *Proceedings of the National Academy of Sciences* **116**, 19875 (2019).

- [16] M. Buzzi, D. Nicoletti, M. Fechner, N. Tancogne-Dejean, M. Sentef, A. Georges, T. Biesner, E. Uykur, M. Dreschel, A. Henderson, T. Siegrist, J. Schlueter, K. Miyagawa, K. Kanoda, M.-S. Nam, A. Ardavan, J. Coulthard, J. Tindall, F. Schlawin, D. Jaksch, and A. Cavalleri, Photomolecular high-temperature superconductivity, *Physical Review X* **10**, 10.1103/physrevx.10.031028 (2020).
- [17] S. Fava, G. De Vecchi, G. Jotzu, M. Buzzi, T. Gebert, Y. Liu, B. Keimer, and A. Cavalleri, Magnetic field expulsion in optically driven yba2cu3o6. 48, *Nature* **632**, 75 (2024).
- [18] Z. Zhang, F. Y. Gao, Y.-C. Chien, Z.-J. Liu, J. B. Curtis, E. R. Sung, X. Ma, W. Ren, S. Cao, P. Narang, A. von Hoegen, E. Baldini, and K. A. Nelson, Terahertz-field-driven magnon upconversion in an antiferromagnet, *Nature Physics* **20**, 788–793 (2024).
- [19] D. Kaplan, P. A. Volkov, A. Chakraborty, Z. Zhuang, and P. Chandra, Tunable spatiotemporal orders in driven insulators, *Physical Review Letters* **134**, 10.1103/physrevlett.134.066902 (2025).
- [20] S. O. Demokritov, V. E. Demidov, O. Dzyapko, G. A. Melkov, A. A. Serga, B. Hillebrands, and A. N. Slavin, Bose–einstein condensation of quasi-equilibrium magnons at room temperature under pumping, *Nature* **443**, 430 (2006).
- [21] P. Nowik-Boltyk, O. Dzyapko, V. E. Demidov, N. G. Berloff, and S. O. Demokritov, Spatially non-uniform ground state and quantized vortices in a two-component bose-einstein condensate of magnons, *Scientific Reports* **2**, 10.1038/srep00482 (2012).
- [22] L. M. Sieberer, M. Buchhold, J. Marino, and S. Diehl, *Universality in driven open quantum matter* (2023), arXiv:2312.03073 [cond-mat.stat-mech].
- [23] S. Sachdev, *Quantum Phase Transitions*, second edition ed. (Cambridge University Press, Cambridge, 2011).
- [24] M. P. A. Fisher, P. B. Weichman, G. Grinstein, and D. S. Fisher, Boson localization and the superfluid-insulator transition, *Physical Review B* **40**, 546 (1989).
- [25] F. Wilczek, Quantum time crystals, *Physical Review Letters* **109**, 160401 (2012).
- [26] A. Shapere and F. Wilczek, Classical time crystals, *Physical Review Letters* **109**, 160402 (2012).
- [27] P. Bruno, Impossibility of spontaneously rotating time crystals: A no-go theorem, *Physical Review Letters* **111**, 070402 (2013).
- [28] H. Watanabe and M. Oshikawa, Absence of quantum time crystals, *Physical Review Letters* **114**, 10.1103/physrevlett.114.251603 (2015).
- [29] V. Khemani, A. Lazarides, R. Moessner, and S. L. Sondhi, Phase structure of driven quantum systems, *Phys. Rev. Lett.* **116**, 250401 (2016), arXiv:1508.03344 [cond-mat.dis-nn].
- [30] D. V. Else, B. Bauer, and C. Nayak, Floquet time crystals, *Physical Review Letters* **117**, 090402 (2016).
- [31] S. Choi, J. Choi, R. Landig, G. Kucsko, H. Zhou, J. Isoya, F. Jelezko, S. Onoda, H. Sumiya, V. Khemani, C. von Keyserlingk, N. Y. Yao, E. Demler, and M. D. Lukin, Observation of discrete time-crystalline order in a disordered dipolar many-body system, *Nature* **543**, 221 (2017), arXiv:1610.08057 [quant-ph].
- [32] J. Zhang, P. W. Hess, A. Kyprianidis, P. Becker, A. Lee, J. Smith, G. Pagano, I.-D. Potirniche, A. C. Potter, A. Vishwanath, N. Y. Yao, and C. Monroe, Observation of a discrete time crystal, *Nature* **543**, 217 (2017), arXiv:1609.08684 [quant-ph].
- [33] N. Y. Yao, C. Nayak, L. Balents, and M. P. Zaletel, Classical discrete time crystals, *Nat. Phys.* **16**, 438 (2020), arXiv:1801.02628 [cond-mat.stat-mech].
- [34] M. P. Zaletel, M. Lukin, C. Monroe, C. Nayak, F. Wilczek, and N. Y. Yao, Colloquium : Quantum and classical discrete time crystals, *Reviews of Modern Physics* **95**, 031001 (2023).
- [35] F. Iemini, A. Russomanno, J. Keeling, M. Schirò, M. Dalmonte, and R. Fazio, Boundary time crystals, *Physical Review Letters* **121**, 035301 (2018).
- [36] O. Scarlatella, R. Fazio, and M. Schirò, Emergent finite frequency criticality of driven-dissipative correlated lattice bosons, *Physical Review B* **99**, 064511 (2019).
- [37] H. Keßler, J. G. Cosme, M. Hemmerling, L. Mathey, and A. Hemmerich, Emergent limit cycles and time crystal dynamics in an atom-cavity system, *Physical Review A* **99**, 053605 (2019).
- [38] P. Kongkhambut, J. Skulte, L. Mathey, J. G. Cosme, A. Hemmerich, and H. Keßler, Observation of a continuous time crystal, *Science* **377**, 670 (2022).
- [39] M. Fruchart, R. Hanai, P. B. Littlewood, and V. Vitelli, Non-reciprocal phase transitions, *Nature* **592**, 363–369 (2021).
- [40] Y. Avni, M. Fruchart, D. Martin, D. Seara, and V. Vitelli, The non-reciprocal ising model, arXiv preprint arxiv:2311.05471 (2024), arXiv:2311.05471 [cond-mat.stat-mech].
- [41] C. P. Zelle, R. Daviet, A. Rosch, and S. Diehl, Universal phenomenology at critical exceptional points of nonequilibrium  $O(n)$  models, *Phys. Rev. X* **14**, 021052 (2024).
- [42] S. Saha, J. Agudo-Canalejo, and R. Golestanian, Scalar active mixtures: The nonreciprocal cahn-hilliard model, *Physical Review X* **10**, 041009 (2020).
- [43] F. Brauns and M. C. Marchetti, Nonreciprocal pattern formation of conserved fields, *Phys. Rev. X* **14**, 021014 (2024).
- [44] T. Suchanek, K. Kroy, and S. A. Loos, Irreversible mesoscale fluctuations herald the emergence of dynamical phases, *Physical Review Letters* **131**, 10.1103/physrevlett.131.258302 (2023).
- [45] R. Hanai, Nonreciprocal frustration: Time crystalline order-by-disorder phenomenon and a spin-glass-like state, *Physical Review X* **14**, 011029 (2024).
- [46] R. Hanai, D. Ootsuki, and R. Tazai, Photoinduced non-reciprocal magnetism, arXiv preprint arXiv:2406.05957 (2024).
- [47] T. Nadolny, C. Bruder, and M. Brunelli, Nonreciprocal synchronization of active quantum spins, arXiv preprint arXiv:2406.03357 (2024).
- [48] A. Kamenev, *Field Theory of Non-Equilibrium Systems* (Cambridge University Press, 2023).
- [49] L. M. Sieberer, M. Buchhold, and S. Diehl, Keldysh field theory for driven open quantum systems, *Reports Prog. Phys.* **79**, 096001 (2016).
- [50] P. C. Martin, E. D. Siggia, and H. A. Rose, Statistical dynamics of classical systems, *Physical Review A* **8**, 423 (1973).
- [51] H.-K. Janssen, On a lagrangean for classical field dynamics and renormalization group calculations of dynamical critical properties, *Zeitschrift für Physik B Condensed Matter and Quanta* **23**, 377 (1976).
- [52] C. De Dominicis, Techniques de renormalisation de la théorie des champs et dynamique des phénomènes cri-

- tiques, *J. Phys. Colloques* **37**, C1 (1976).
- [53] E. Fradkin, *Field Theories of Condensed Matter Physics*, 2nd ed. (Cambridge University Press, 2013).
  - [54] N. Walldorf, D. M. Kennes, J. Paaske, and A. J. Millis, The antiferromagnetic phase of the floquet-driven hubbard model, *Phys. Rev. B* **100**, 121110 (2019).
  - [55] M. H. Kalthoff, D. M. Kennes, A. J. Millis, and M. A. Sentef, Nonequilibrium phase transition in a driven-dissipative quantum antiferromagnet, *Phys. Rev. Res.* **4**, 023115 (2022).
  - [56] R. Daviet, C. P. Zelle, A. Rosch, and S. Diehl, Nonequilibrium criticality at the onset of time-crystalline order, *Phys. Rev. Lett.* **132**, 167102 (2024).
  - [57] R. Hanai, A. Edelman, Y. Ohashi, and P. B. Littlewood, Non-hermitian phase transition from a polariton bose-einstein condensate to a photon laser, *Physical Review Letters* **122**, 185301 (2019).
  - [58] T. Risler, J. Prost, and F. Jülicher, Universal critical behavior of noisy coupled oscillators, *Phys. Rev. Lett.* **93**, 175702 (2004).
  - [59] T. Risler, J. Prost, and F. Jülicher, Universal critical behavior of noisy coupled oscillators: A renormalization group study, *Physical Review E* **72**, 016130 (2005).
  - [60] L. M. Sieberer, S. D. Huber, E. Altman, and S. Diehl, Dynamical Critical Phenomena in Driven-Dissipative Systems, *Phys. Rev. Lett.* **110**, 195301 (2013).
  - [61] U. C. Täuber and S. Diehl, Perturbative field-theoretical renormalization group approach to driven-dissipative bose-einstein criticality, *Phys. Rev. X* **4**, 021010 (2014), [arXiv:1312.5182 \[cond-mat.stat-mech\]](#).
  - [62] S. M. Rezende, Theory of coherence in bose-einstein condensation phenomena in a microwave-driven interacting magnon gas, *Physical Review B* **79**, 174411 (2009).
  - [63] R. Daviet, C. P. Zelle, A. Asadollahi, and S. Diehl, Kardar-parisi-zhang scaling in time-crystalline matter, *arXiv preprint arXiv:2412.09677* [10.48550/ARXIV.2412.09677](#) (2024).
  - [64] D. Hardt, R. Doostani, S. Diehl, N. Del Ser, and A. Rosch, Propelling ferrimagnetic domain walls by dynamical frustration, *Nature Communications* **16**, 3817 (2025).

# Supplemental Material: Nonequilibrium condensates in parametrically pumped field theories

## 1. ELIMINATION OF HIGH FREQUENCY BATH

In this appendix we give the details on the elimination of the highly occupied reservoir modes at large momenta  $q_\Omega$ , which we call the fast modes  $\phi_>$ . To that end, we assume that the occupation of modes is peaked at these momenta, so that we can write the occupation function as  $n(q) \approx \delta(q - q_\Omega) \cdot n_b$ , where  $n_b$  is the number of modes that the pump injects at the resonant momentum  $q_\Omega$  and increases with pump power.

Our goal is to derive the corrections to the response as well as occupation functions of the low frequency regime that arise by eliminating the fast reservoir modes  $\phi_>$ . We will do this in a perturbative diagrammatic approach using nonequilibrium Green functions, or equivalently a perturbative expansion of the MSRJD path integral [S1].

For our model, (3), the bare retarded and advanced responses have the form

$$\chi_{ij}^{R/A}(\omega, \mathbf{q}) = G^{R/A}(\omega, \mathbf{q}) \delta_{ij} = \frac{\delta_{ij}}{-\omega^2 \pm i\omega\gamma(\mathbf{q}) + r(\mathbf{q})}, \quad (\text{S1})$$

where  $i, j = 1, \dots, N$  for an  $O(N)$  symmetric theory and we expand the momentum dependencies of the damping as well as the gap text as

$$\gamma(\mathbf{q}) = \gamma + Z_1 \mathbf{q}^2, \quad r(\mathbf{q}) = r + Z_2 \mathbf{q}^2. \quad (\text{S2})$$

The correlation function is

$$\langle \phi_i(\omega, \mathbf{q}) \phi_j(-\omega, -\mathbf{q}) \rangle = \mathcal{C}_{ij}(\omega, \mathbf{q}) = G^K(\omega, \mathbf{q}) \delta_{ij}, \quad G^K(\omega, \mathbf{q}) =: f(\omega, \mathbf{q}) G^R(\omega, \mathbf{q}) G^A(\omega, \mathbf{q}). \quad (\text{S3})$$

Using the occupation of the reservoir modes, we can fix the correlation function  $G_>^K$  of the reservoir

$$n(\mathbf{q}) = \int_{\omega} G_>^K(\omega, \mathbf{q}) \quad (\text{S4})$$

to wit

$$f(\omega, \mathbf{q}) = n_b \delta(|\mathbf{q}| - q_\Omega) \gamma(\mathbf{q}). \quad (\text{S5})$$

The antidamping impact on the slow modes is given by the self-energy contributions  $\Sigma_p$  stemming from integrating out  $\phi_>$ , i.e. all internal loop correlation functions are associated to the fast fields  $\phi_>$ . The shift of the damping is encoded in the corrections to the retarded response, i.e.  $\delta\gamma = \text{Im} \partial_\omega \Sigma_p^R(\omega = 0, \mathbf{q} = 0)$ . The heating effect is encoded in the correction to the inverse correlation  $\Delta D = \Sigma_p^K(\omega = 0, \mathbf{q} = 0)$ . Below, we derive these corrections perturbatively.

*Antiferromagnet* – In the case of an antiferromagnet, where  $\kappa = 0$  and the scattering vertex is the quartic  $\lambda\phi^4$  coupling. The leading order contribution to the frequency dependence of  $\Sigma_p^R$  is the two-loop sunset diagram stemming from the  $\lambda\phi^4$  coupling. The loop integral reads

$$I_{\text{sunset}}(\omega, \mathbf{q} = 0) = (2\pi)^{-2d-2} \int_{\mathbf{q}_1, \mathbf{q}_2, \mathbf{q}_3} \int_{\omega_1, \omega_2, \omega_3} \delta(\omega_1 + \omega_2 + \omega_3 + \omega) \delta(\mathbf{q}_1 + \mathbf{q}_2 + \mathbf{q}_3) G_>^K(\omega_1, \mathbf{q}_1) G_>^K(\omega_2, \mathbf{q}_2) G^R(\omega_3, \mathbf{q}_3). \quad (\text{S6})$$

Using a Fourier representation of the  $\delta$  distributions, we rewrite

$$I_{\text{sunset}}(\omega, 0) = (2\pi)^{-3d-3} \int_{\mathbf{s}, t} e^{it\omega} \left( \int_{\mathbf{q}_1, \omega_1} e^{i\mathbf{s} \cdot \mathbf{q}_1 + it\omega_1} G_>^K(\omega_1, \mathbf{q}_1) \right) \quad (\text{S7})$$

$$\left( \int_{\mathbf{q}_2, \omega_2} e^{i\mathbf{s} \cdot \mathbf{q}_2 + it\omega_2} G_>^K(\omega_2, \mathbf{q}_2) \right) \left( \int_{\mathbf{q}_3, \omega_3} e^{i\mathbf{s} \cdot \mathbf{q}_3 + it\omega_3} G^R(\omega_3, \mathbf{q}_3) \right). \quad (\text{S8})$$



Now we use rotational invariance of the Greens functions, i.e. that they only depend on  $q \equiv |\mathbf{q}|$  and restrict ourselves to  $d = 3$  to perform the angular momentum integrations. To this end we use

$$\int d^3 \mathbf{q} e^{i\mathbf{s} \cdot \mathbf{q}} F(q) = 2\pi \int_{-\infty}^{\infty} q^2 dq \frac{\sin qs}{qs} F(q), \quad (\text{S9})$$

where  $s = |\mathbf{s}|$ . We can now straightforwardly perform the integration over  $\mathbf{s}$  by  $\int d^3 \mathbf{s} s^{-3} \sin^3(sq_\Omega) = \pi^2$ . We then compute the subintegrals  $I_1 = \int d\omega \int q dq e^{it\omega} G^R(\omega, q)$  and  $I_2 = \int d\omega \int q dq e^{it\omega} G_{>}^K(\omega, q)$ . Since  $G^R$  has poles in the lower complex half plane only,  $I_1$  is proportional to  $\theta(-t)$ . Performing the frequency as well as momentum integration yields

$$I_1 = \frac{4e^{\gamma t} \pi^2 \arctan Z_2/Z_1}{Z_2} \theta(-t). \quad (\text{S10})$$

For  $I_2$  we can use the momentum shell constraint of (S5) to wit, for  $t < 0$

$$I_2 = 4\pi q_\Omega \delta q n_b \int_{\omega} e^{it\omega} \frac{2i\gamma_\Omega}{(\gamma_\Omega^2 + (\omega - \Omega)^2)(\gamma_\Omega^2 + (\omega + \Omega)^2)} = -\frac{4\pi q_\Omega n_b e^{\gamma_\Omega t} (\gamma_\Omega \sin \Omega t - \Omega \cos \Omega t)}{\Omega}, \quad (\text{S11})$$

where  $\gamma_\Omega$  is the decay rate into the bath of excitations at  $q_\Omega$ . In three dimensions, we thus arrive at

$$I_{\text{sunset}}(\omega, 0) = 2^{-6} \pi^{-3} \int_{-\infty}^{\infty} dt e^{i\omega t} I_1 I_2^2. \quad (\text{S12})$$

We are only interested in the frequency derivative at  $\omega = 0$ :

$$\partial_\omega I_{\text{sunset}}(\omega = 0, \mathbf{q} = 0) = 2^{-6} \pi^{-3} \int_{-\infty}^{\infty} dt it I_1 I_2^2. \quad (\text{S13})$$

This integral can be performed analytically. For  $\Omega \gg \gamma_\Omega \gg \gamma$  it yields

$$\partial_\omega I_{\text{sunset}}(\omega = 0, \mathbf{q} = 0) \approx -i \frac{(q_\Omega n_b)^2 \arctan Z_2/Z_1}{256 Z_2 \gamma_\Omega^2} \quad (\text{S14})$$

The full self energy contains additional factors of  $(\lambda/4)^2$ , the bare scattering of the original theory, a combinatorial factor of  $2 \cdot 3$  and a factor  $N$  from the traces over the internal  $O(N)$  indices and thus

$$\partial_\omega \Sigma_p^R(\omega = 0, \mathbf{q} = 0) = \frac{3N\lambda^2}{8} \partial_\omega I_{\text{sunset}}(\omega = 0, \mathbf{q} = 0). \quad (\text{S15})$$

Therefore, the shift of the damping for the antiferromagnet ( $N = 3$ ) to leading order in perturbation theory is

$$\delta\gamma = \text{Im} \partial_\omega \Sigma_p^R(\omega = 0, \mathbf{q} = 0) \approx -\mathcal{N}_\gamma \frac{(q_\Omega n_b)^2}{\gamma_\Omega^2} < 0, \quad (\text{S16})$$

proving that the pumping effectively leads to an antidamping contribution. Here  $\mathcal{N}_\gamma = \frac{\arctan Z_2/Z_1}{256 Z_2}$ .

Equivalently, the pumped bath will also lead to a noise increase  $\Delta D$  in the low energy modes that will counteract ordering instabilities. This also manifests in a self energy contribution stemming from a sunset diagram with three internal Keldysh Green functions,

$$\Delta D = N\lambda^2 2^{-5} \pi^{-3} \int_{-\infty}^0 dt I_2^3 \approx \frac{5(q_\Omega n_b)^3}{32\Omega^2}, \quad (\text{S17})$$

where we symmetrised the  $t$  integration which initially runs from  $-\infty$  to  $\infty$  and again used  $\gamma_\Omega \ll \Omega$ .

*Ferromagnet* In the case of a ferromagnet, there is an interaction  $\kappa\epsilon_{ijk}\tilde{\phi}_i\partial_t\phi_j\phi_k$  and thus the leading contribution to  $\partial_\omega\Sigma_p^R$  stems from a one loop integral. Here, care needs to be taken when contracting the antisymmetric vertices. The configuration in which the time derivative of the vertex hits an external leg leads to a contribution to the damping

$$\kappa^2\epsilon_{ijk}\frac{1}{(2\pi)^4}(\epsilon_{jik}+\epsilon_{kij})\int_{\omega,\mathbf{q}}(-i\omega)G^R(\mathbf{q},\omega)G_{>}^K(\mathbf{q},\omega)=0. \quad (\text{S18})$$

The remaining contributions are

$$\begin{aligned} \partial_\omega\Sigma_p^R &= \frac{\kappa^2}{(2\pi)^4}\partial_\omega\bigg|_{\omega=0}\epsilon_{ijk}\left(\epsilon_{kji}\int_{\nu,\mathbf{q}}(-i(\nu-\omega))^2G_{>}^K(\nu-\omega,\mathbf{q})G^R(\nu,\mathbf{q})\right. \\ &\quad \left.+ \epsilon_{jki}(-i(\nu-\omega))G_{>}^K(\nu-\omega,\mathbf{q})(-i\nu)G^R(\nu,\mathbf{q})\right) \\ &= -\kappa^2\int_{\nu,\mathbf{q}}\nu G_{>}^K(\nu,\mathbf{q})G^R(\nu,\mathbf{q}) = -i\kappa^2\frac{n_b q_\Omega^2 \delta q}{4\pi^3 \gamma_\Omega}. \end{aligned} \quad (\text{S19})$$

As above, we have established, that the slow spin waves experience an effective antidamping contribution due to the reservoir modes.

Similarly to the case of the antiferromagnet, there is also a self energy contribution to the noise, which reads

$$\Delta D = 2\kappa^2\int_{\omega,\mathbf{q}}G_{>}^K(\omega\mathbf{q})^2 \approx \frac{(n_b q_\Omega^2 \delta q)^2}{2\pi\gamma_\Omega}. \quad (\text{S20})$$

### Nonlinear dampings

The nonlinear damping contributions to the MSRJD Lagrangian  $u(\tilde{\phi}\cdot\partial_t\phi)(\phi\cdot\phi)$  and  $u'/2(\tilde{\phi}\cdot\phi)\partial_t(\phi\cdot\phi)$  are crucial to stabilize the limit cycle phases. Since they are RG relevant in the vicinity of the transition into the rotating and oscillating phases below four dimensions, as the prior analysis showed [S41, S56], we expect them to be generated as soon as symmetries allow them upon coarse graining close to the antidamping instability. Here we show explicitly how they are generated on the one-loop level as above.

To that end we first look at the full frequency dependence, at vanishing external momenta, of the vertex in leading order perturbation theory

$$\begin{aligned} \Gamma^{(13)}(\omega_1,\omega_2,\omega_3) &= \frac{\delta^4\Gamma}{\delta\tilde{\phi}_a(-\sum\omega_i)\phi_a(\omega_1)\phi_b(\omega_2)\phi_b(\omega_3)} = \lambda - \lambda^2(2\pi)^{-d-1}\int_{\mathbf{q},\omega}\left(N^2G_{>}^K(\omega-\omega_2-\omega_3,\mathbf{q})G^R(\omega,\mathbf{q})\right. \\ &\quad \left.+ G_{>}^K(\omega-\omega_1-\omega_3,\mathbf{q})G^R(\omega,\mathbf{q}) + G_{>}^K(\omega-\omega_1-\omega_2,\mathbf{q})G^R(\omega,\mathbf{q})\right) + \mathcal{O}(\lambda^3) \end{aligned} \quad (\text{S21})$$

Now, we identify

$$u = i\partial_{\omega_1}\Gamma^{(13)}(\omega_1,\omega_2,\omega_3)\big|_{\omega_i=0}, \quad (\text{S22})$$

$$u' = \frac{i}{2}(\partial_{\omega_2}+\partial_{\omega_3})\Gamma^{(13)}(\omega_1,\omega_2,\omega_3)\big|_{\omega_i=0}, \quad (\text{S23})$$

to find that

$$u = i\frac{2\lambda^2}{(2\pi)^{d+1}}\int_{\mathbf{q},\omega}(\partial_\omega G_{>}^K(\omega,\mathbf{q}))G^R(\omega,\mathbf{q}) + \mathcal{O}(\lambda^3), \quad (\text{S24})$$

$$u' = i\frac{(N^2+1)\lambda^2}{(2\pi)^{d+1}}\int_{\mathbf{q},\omega}(\partial_\omega G_{>}^K(\omega))G^R(\omega,\mathbf{q}) + \mathcal{O}(\lambda^3). \quad (\text{S25})$$

The loop integral over the reservoir Green's functions can be performed straightforwardly, in the same manner as in the self energy contributions and we find

$$u = \frac{\lambda^2(\Omega^2 + 5\gamma_\Omega^2)q_\Omega^2 n_b \delta q}{4\gamma_\Omega(\Omega^2 + \gamma_\Omega^2)^2(2\pi)^3} > 0. \quad (\text{S26})$$

$$u' = \frac{N^2+1}{2}u \quad (\text{S27})$$

We thus have established, that the nonlinearities stabilizing the limit cycle phases are generated with the correct signs by integrating out the pumping reservoir. Furthermore, we showed that  $u' > u$  in leading order perturbation theory and the system will go into the rotating phase rather than showing amplitude oscillations [S41].

## 2. UNIVERSAL SCALING IN THE PRESENCE OF FERROMAGNETIC COUPLING.

Here we consider the case of an  $SO(3)$  but not  $O(3)$  symmetric theory. This is e.g. a ferromagnet in contrast to a Heisenberg antiferromagnet, where the  $\mathbb{Z}_2$  redundancy of the Néel vector causes the system to be fully  $O(3) = \mathbb{Z}_2 \ltimes SO(3)$  symmetric. The coupling distinguishing those two cases is the precessing force term  $\sim \kappa$ , see Eq. (7). For larger  $N$ , the difference between  $SO(N)$  and  $O(N)$  is encoded in higher order couplings which are irrelevant at the transitions.

For only  $SO(3)$  symmetry, the transition between paramagnet and time crystal is described by the nonthermal  $O(3) \times SO(2)$  universality class recently found in [S56]. The transition between ferromagnet and time crystal is instead described by the universality class of the noisy Hopf bifurcation [S1, S58], as we will demonstrate now.

### 2.1 Ferromagnet to time crystal

We start with the ordered phase in the presence of the ferromagnetic coupling  $\kappa$ . Without loss of generality, we assume the magnetic order to be oriented along the  $z$  axis and expand fluctuations around the mean-field solution  $\phi = (m_1, m_2, \sigma + \sigma_0)$ . The longitudinal fluctuations  $\sigma_0$  are gapped and we restrict ourselves to the dynamics of the Goldstone modes  $m_{1,2}$ . It is useful to collect the two Goldstone modes into one complex field  $m = m_1 + im_2$  and switch to a phase-space description of dynamics by introducing the corresponding conjugate field  $\pi = \partial_t m$ . Linearizing the field theory around the static order in this basis yields

$$\partial_t \pi + (\delta + i\sigma_0 \kappa - Z\nabla^2)\pi - Z\nabla^2 m + \xi = 0, \quad (\text{S28})$$

$$\partial_t m = \pi. \quad (\text{S29})$$

Since  $m$  is a Goldstone mode it has to be gapless. This implies that  $m$  can only appear with derivatives acting on it. Further, the dynamics has to be invariant under the unbroken subgroup  $U(1)$ . Here,  $\delta = 2\gamma + u\sigma_0^2$  is the tuning parameter that triggers the transition between static ( $\delta > 0$ ) and rotating ( $\delta < 0$ ) phase, which spontaneously breaks the  $U(1)$  group. Eq. (S28) reveals that the universal fluctuations are captured by a noisy Hopf bifurcation of the conjugate momentum  $\pi$  coupled to the gapless Goldstone modes  $\text{Re } m, \text{Im } m$ . The finite frequency  $\kappa\sigma_0 \neq 0$  at which the Hopf bifurcation takes place is induced by  $\kappa \neq 0$  and prevents the transition from occurring through a critical exceptional point, which would render it first order. This is a consistent mean field picture of a precession, at the transition we see a finite frequency condensation of the conjugate spin wave momentum  $\vec{\pi} = \pi_0(\cos \sqrt{\sigma_0 \kappa t}, \sin \sqrt{\sigma_0 \kappa t}, 0)^T$ . Plugging this back into  $\vec{\phi} = (m_1, m_2, \sigma + \sigma_0)$ ,  $\partial_t \vec{\phi} = \vec{\pi}$  yields exactly the precessing phase from 3.

The decoupling of the critical mode  $\pi$  from the soft diffusive Goldstone mode  $m$  occurs through their frequency separation. To study the universal fluctuations of the critical mode, we transform into its rotating frame,  $\pi \rightarrow e^{iEt}\pi$ ,  $m \rightarrow e^{iEt}m$  with  $E = \sigma_0 \kappa$ . This gives a mass-like contribution to the mode  $m$  and, it thus can be integrated out adiabatically, since it moves much faster than the critical mode. This exactly reproduces a noisy Gross-Pitaevskii equation for  $\pi$  in the rotating frame,

$$\partial_t \pi + \delta \cdot \pi + (Z_1 - iZ_2/E)\nabla^2 \pi + \xi_\pi = 0. \quad (\text{S30})$$

Including the relevant, symmetry-allowed interactions reproduces a complex Gross-Pitaevskii equation (cGPE). This shows that the universal exponents of the transition between ferromagnet and time-crystal are described by the Hopf or cGPE universality class [S58, S60, S61].